

## **STUDIES ON LOADING, CRACKING AND CLUSTERING OF PARTICULATES ON THE STRENGTH AND STIFFNESS OF 7020/SiC<sub>p</sub> METAL MATRIX COMPOSITES**

**A. CHENNAKESAVA REDDY**

Professor, Department of Mechanical Engineering, JNTUH College of Engineering,  
Kukatpally, Hyderabad, Telangana, India

### **ABSTRACT**

The objective of this work is to study the influence of volume fraction, size of particulates, formation of precipitates at the matrix/particle interface, particle cracking, voids/porosity, and clustering of particulates on the strength and stiffness of 7020/SiC<sub>p</sub> metal matrix composites. Tensile strength and stiffness, increase with an increase in the volume fraction of SiC particulates. The tensile strength and stiffness decrease with increase in size of the particulates, presence of porosity, clustering, and particle cracking. Clustering is more prominent in the composites having very small-reinforced particulates. Mg<sub>2</sub>Si and MgZn<sub>2</sub> compound are likely to precipitate at the matrix/particle interfaces of 7020/SiC composite.

**KEYWORDS:** 7020, Tensile Strength, SiC, Clustering, Particle Cracking, Porosity, Interface Bonding

### **INTRODUCTION**

The 7020 alloy is composed of 99.0 weight percentage aluminium and 1.0 weight percentage zinc. This material is used as cladding material on the coolant side of heat exchanger components. 7020 is an attractive and viable candidate for aircraft and aerospace applications for its excellent resistance to stress corrosion cracking on exposure to the atmosphere. Reinforcement by particulates of SiC has proved to be exclusively beneficial since it offers the metal matrix composites having nearly isotropic mechanical properties at low price. Notwithstanding their exceptional mechanical properties, Al-SiC composites fabricated through casting route, suffer disadvantageous effects such as sedimentation of particulates, higher porosity level, poor wettability, clustering and cracking of particulates and interfacial reactions as mentioned by Rohatgi et al. (1986) and Reddy (2011). Lee et al. (1994) have observed that the SiC particulates detach from the aluminium matrix during tensile loading. Prakash et al. (1995) have concluded that a poor adhesion between particle and matrix may lead to local yielding owing to change of local stress state at the particle-matrix interface. On that point are some methods of improving the wettability of reinforced particulates in the metal matrix composites. The wettability of SiC particulates can be enhanced by coating techniques using Ni, Cu, and Si as stated by Hashim et al. (2001). In contrast, Cu deteriorates wetting; Si improves wettability at temperature higher than 1000°C. Laurent et al. (1987) have adopted preheating of SiC particulates before addition into liquid Al. In cast metal-matrix composites, particle clustering is unavoidable because of the pooled effect of particulate sedimentation and refusal of the particulate by the matrix dendrites during solidification as observed by Vaucher & Beffort (2001). An additional possibility of particle clustering is very common with small particulates in the metal matrix composites as quantified by Reddy (2009). All these phenomena may influence the tensile strength and stiffness of composite.

The objective of this study is to examine the volume fraction and particle size of SiC<sub>p</sub>, clustering and cracking of

particulates, voids/porosity, and formation of precipitates at the particle/matrix interface on the tensile strength and stiffness of 7020/SiCp metal matrix composites.

## WEIBULL MODEL TO FIND THE RELIABILITY OF COMPOSITES

The Weibull cumulative distribution to find reliable strength of composite is presented by:

$$F(x) = 1 - e^{-\left(\frac{x}{\alpha}\right)^\beta} \quad (1)$$

$$\ln\left[\ln\left(\frac{1}{1-F(x)}\right)\right] = \beta \ln x - \beta \ln \alpha = mx + c \quad (2)$$

where  $m$  is the slope of a straight line and  $c$  is the intercept. So, when we perform the linear regression, the shape parameter ( $\beta$ ) comes directly from the slope of the line. The scale parameter ( $\alpha$ ) must be calculated as follows:

$$\alpha = e^{\left(-\frac{c}{\beta}\right)} \quad (3)$$

According to the Weibull statistical-strength theory for brittle materials, the probability of survival,  $P$  at a maximum stress ( $\sigma$ ) for uniaxial stress field in a homogeneous material governed by a volumetric flaw distribution is given by

$$P(\sigma_f \geq \sigma) = R(\sigma) = e^{-B(\sigma)} \quad (4)$$

where  $\sigma_f$  is the value of maximum stress of failure,  $R$  is the reliability, and  $\beta$  is the risk of rupture. For a two-parameter Weibull model, the risk of rupture is of the form

$$B(s) = A \left( \frac{\sigma_f}{\sigma_0} \right)^\beta \quad (\sigma_0, \beta > 0) \quad (5)$$

where  $\sigma_0$  is the characteristic strength, and  $\beta$  is the shape factor. The author has proposed expression for the tensile strength considering the effects of reinforced particle size and porosity. The expression of tensile strength is presented under:

$$\text{Tensile strength, } \sigma_t = \sigma_o [V_m + V_p - V_v]^{-1/\beta} \quad (\sigma_0, \beta_t > 0) \quad (6)$$

where  $V_m$ ,  $V_p$ , and  $V_v$  are respectively volume of the matrix, volume of the reinforced particles and volume of the porosity in the tensile specimen.

## MATERIALS AND METHODS

The materials used in this work were 7020 matrix alloy silicon carbide particulates (SiC<sub>p</sub>). The volume fractions of SiC<sub>p</sub> reinforcement are 12%, 16%, and 20%. The particle sizes of SiC<sub>p</sub> reinforcement are 800 nm, 10  $\mu$ m, and 20  $\mu$ m.

### Preparation of Melt and Metal Matrix Composites

7072 matrix was melted in a resistance furnace. A graphite crucible was used to melt the metal. The 7072 was cut into little pieces and placed into the crucible to form a bottom layer of the ground substance. The melting losses of the alloy constituents were involved into account while fixing the complaint. Then SiC particles (as per volume fraction required in the composite) were carefully laid on top of this layer mitigating the drop of particles to the underside of the crucible. After that, other pieces of 7072 were placed above the particles to ensure scattering of the particles in the bulk. The whole crucible was then heated. During the melting process, the charge was fluxed with coverall to prevent dressing. The molten alloy was degasified by tetrachlorethane (in solid shape). The crucible was taken off from the furnace and treated with sodium modifier. Then the liquid melt was allowed to cool down just below the liquidus temperature to get the melt semi solid state. At this stage, the preheated (500<sup>0</sup>C for 1 hour) SiC particles were added to the liquid melt. The molten alloy and SiC particles are thoroughly stirred manually for 15 minutes. After manual steering, the semisolid liquid melt was reheated to a full liquid state in the resistance furnace followed by an automatic mechanical stirring using a mixer to make the melt homogenous for about 10 minutes at 200 rpm. The temperature of melted metal was measured using a dip type thermocouple. The preheated cast iron die was filled with dross-removed melt by the compressed (3.0 bar) argon gas as conducted by Reddy & Essa (2010, 2011).

### Heat Treatment

Prior to the machining of composite samples, a solution treatment was applied at 500<sup>0</sup>C for 8 hours, followed by quenching in cold water at 30<sup>0</sup> C. The samples were then naturally aged at room temperature for 5 hours. The samples were given precipitation treatment by keeping in the furnace 165<sup>0</sup>C for 8 hours.

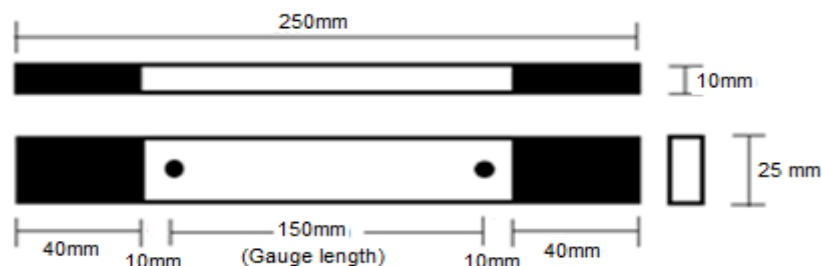


Figure 1: Dimensions of Flat Tensile Specimen



Figure 2: Tensile Testing of Metal Matrix Composite

### Tensile Tests

The heat-treated samples were machined to get flat-rectangular specimens (Figure1) for the tensile tests.

The tensile specimens were placed in the grips of a Universal Test Machine (UTM) at a specified grip separation and pulled until failure as shown in Figure 2. The test speed was 2 mm/min (as for ASTM D3039). The load v/s displacement curve was obtained from the computer interfaced with the UTM.

### Optical and Scanning Electron Microscopic Analysis

An image analyzer was used to study the distribution of the reinforcement particles within the 7020aluminum alloy matrix. The polished specimens were ringed with distilled water and were etched with 0.5% HF solution for optical microscopic analysis. Fracture surfaces of the deformed/fractured test samples were analyzed with a scanning electron microscope (S-3000N Toshiba SEM) to define the macroscopic fracture mode and to establish the microscopic mechanisms governing fracture.

## RESULTS AND DISCUSSIONS

The elasticity modulus is the measure of stiffness. The tensile strength is the maximum stress that the material can sustain under a uniaxial loading. The characteristic parameters like volume fraction of particles, particle size, matrix/particle interface bonding, agglomeration of particles, particle cracking, formation of precipitates, and voids/porosity that influence the strength and stiffness of 7020/SiCp metal matrix composite are discussed in the following sections.

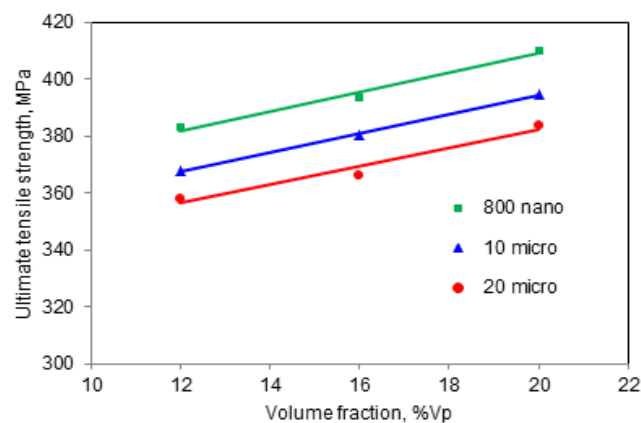


**Figure 3: Variation of the Tensile Strength with the Volume Fraction and Particle Size of SiCp**

### Cause of Strengthening Mechanism in 7020/SiC Composite

The effect of volume fraction and particle size on tensile strength with is presented in Figure 3. It is shown that, for a given particle size the tensile strength increases with an increase in the volume fraction of SiCp. The tensile strength decreases with an increase in the particle size. Lloyd (1991) has studied that the strengthening mechanism in the particulate dispersed metal matrix composite is because of obstruction to the movement of dislocations and the deformation of material [14]. The amount of obstruction to the dislocations is high for small particles. The other possibility, of increasing strength is due to the formation of precipitates at the particle/matrix interface. There is an acceleration of nucleation and growth of precipitates in 7020/SiC/20 $\mu$ m and 7020/SiC/10 $\mu$ m but that there is only an acceleration of growth in 7020/SiC/800nm. The precipitates that are formed 7020/SiC/800nm are Mg<sub>2</sub>Si, MgZn<sub>2</sub>, Al<sub>6</sub>Si, and Al<sub>3</sub>Fe as shown in Figure 4. The precipitation of MgZn<sub>2</sub> is observed at the particle/matrix interface as shown in Figure 5a. The precipitation of MgZn<sub>2</sub> at interface during heat treatment is shown in Figure 5b.

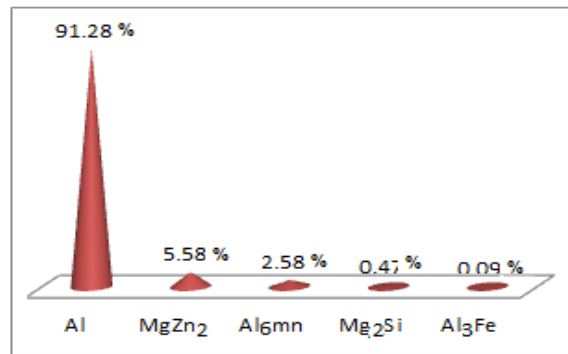


Figure 4: Precipitates in 7020/SiC

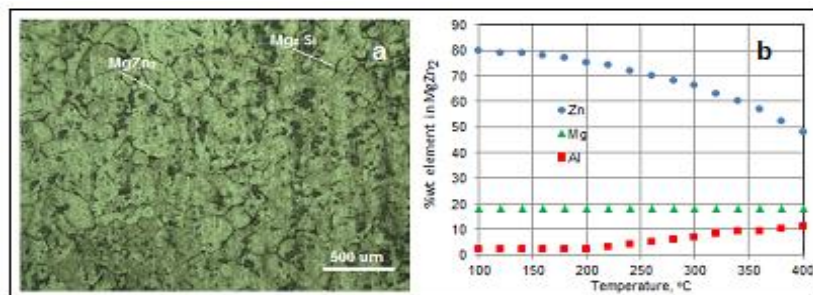


Figure 5: Formation of Precipitates in 7020/SiC Composite (SiC Particle Size = 800nm and vp = 30%)

### Catastrophe of Strengthening Mechanism in 7020/SiC Composite

Non-planar cracking of particle (Figure 6) is observed in the 7020/SiCp composite comprising 20 $\mu$ m particles. For composite of 20% volume fraction and 800nm, the tensile strength was 410.20 MPa. For composite of 20% volume fraction and 20 $\mu$ m, the tensile strength was 353.60 MPa. The decrease in tensile strength was 56.60 MPa. This is because of difference in the passion's ratio of SiC particle 7020 matrix alloy. There is every possibility of cavity formation during the preparation of composite or during testing of composite due to debonding as reported Whitehouse & Clyne (1993). The particle debonding is observed at the interface of particle/matrix as shown in Figure 7a. The porosity of approximately 36 $\mu$ m was also revealed in the 7020/SiCp composite having 20 $\mu$ m particles as shown in Figure 7b. The clusters act as sites of stress concentration. The formation of clustering increases with an increase in the volume fraction and with a decrease in the particle size. Some clusters of smaller particles can be viewed in the untreated filler composite as shown in Figure 8.

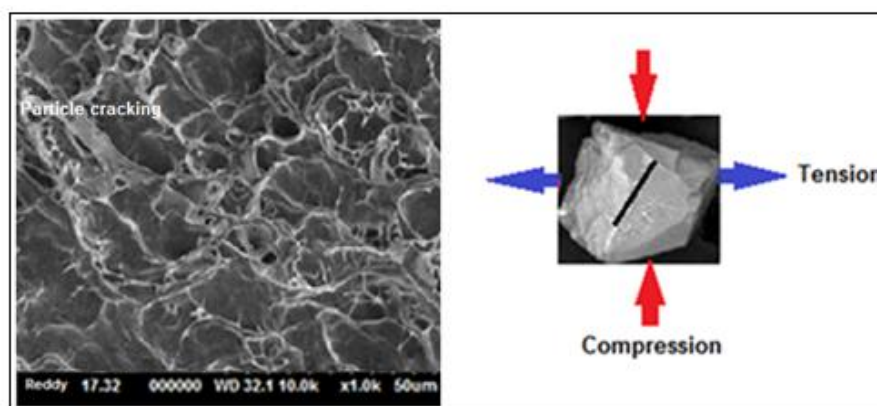
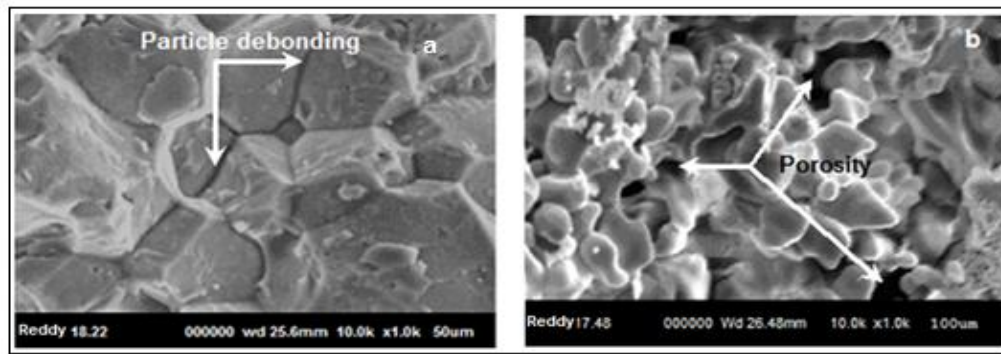
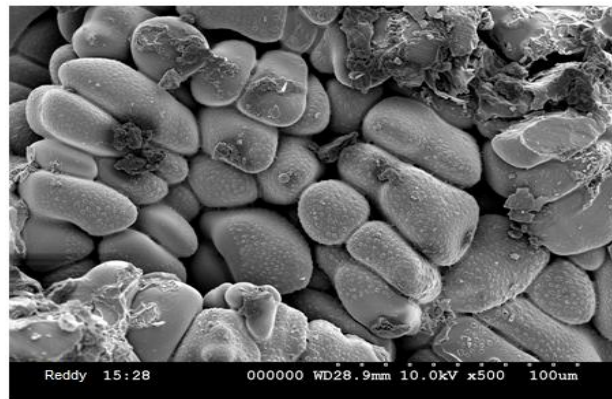


Figure 6: Particle Cracking due to Tensile Loading



**Figure 7: Cavity Formation (a) Debonding due to Tensile Loading and (b) Porosity in Untested Specimen**



**Figure 8: Clustering of Particles**

### Theories of Strengthening Mechanisms

The strength of a particulate composite depends on the strength of the weakest zone and metallurgical phenomena in it. Pukanszky et al. (1998) presented an empirical relationship for very strong particle-matrix interfacial bonding, as given below:

$$\sigma_c = \left[ \sigma_m \left( \frac{1 - \nu_p}{1 + 2.5\nu_p} \right) \right] e^{B\nu_p} \quad (7)$$

where  $B$  is an empirical constant, which depends on the surface area of particles, particle density and interfacial bonding energy. The value of  $B$  varies between from 3.49 to 3.87. This criterion has taken care of the presence of particulates in the composite and interfacial bonding between the particle/matrix. The trend of variation of tensile strength is same as experimental results as shown in Figure 9. Nevertheless, the issue of particle size and voids/porosity were not studied in this standard.

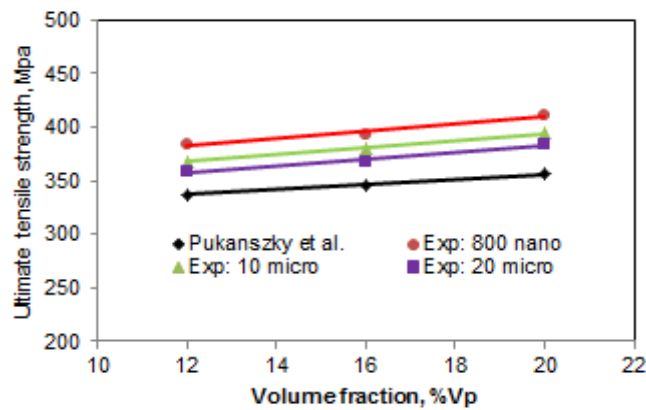


Figure 9: Comparison of Pukanszky et al Criterion with Experimental Values

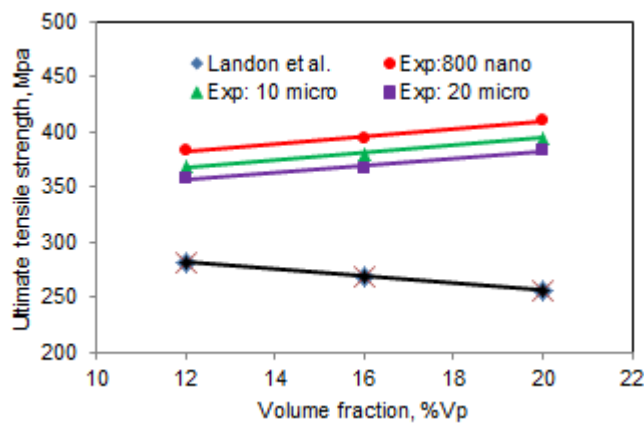


Figure 10: Comparison of Landon et al Criterion with Experimental Values

An empirical linear relationship between composite strength and particle size was proposed by Landon et al. (1977):

$$\sigma_c = \sigma_m(1 - v_p) - k(v_p)d_p \quad (8)$$

where  $k(v_p)$  is the gradient of the tensile strength against the mean particle size (diameter) and is a function of particle volume fraction  $v_p$ . This criterion is applicable to poorly bonded micro-molecules, but cannot apply to strong interfacial adhesion. The tensile strength decreases with an increase in the volume fraction. This criterion does not follow the trend of the experimental results as shown in Figure10.

Hojo et al. (1974) found that the strength of a composite varies linearly with the mean particle size  $d_p$  according to the relation

$$\sigma_c = \sigma_m + k(v_p)d_p^{-1/2} \quad (10)$$

where  $k(v_p)$  is a constant being a function of the particle loading. This criterion fails for larger particles as shown in Figure 11. However, the composite strength decreases with increasing filler loading in the composite.



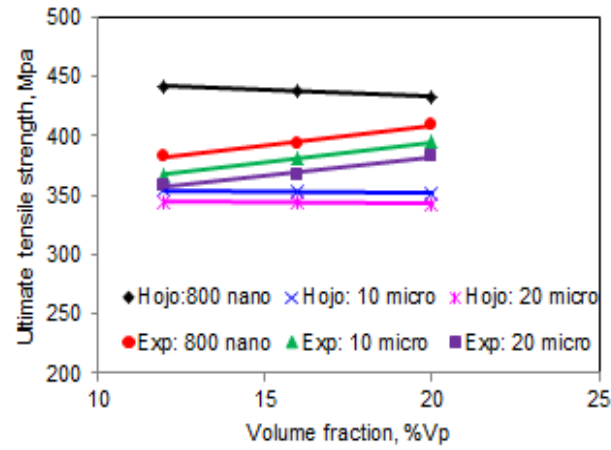


Figure 11: Comparison of Hojo Criterion with Experimental Values

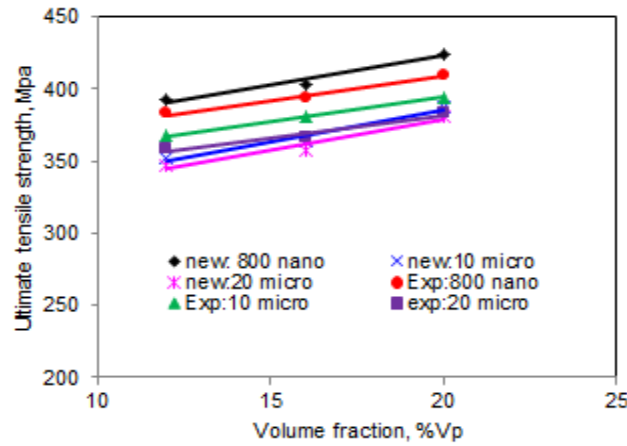


Figure 12: Comparison of Proposed Criterion with Experimental Values

A new criterion is suggested by the author considering adhesion, formation of precipitates, particle size, agglomeration, voids/porosity, obstacles to the dislocation, and the interfacial reaction of the particle/matrix. The formula for the strength of composite is stated below:

$$\sigma_c = \left[ \sigma_m \left( \frac{1 - (v_p + v_v)^{2/3}}{1 - 2(v_p + v_v)} \right) \right] e^{m_m(v_p + v_v)} + k(v_p) m_p d_p^{-1/2} \quad (11)$$

where  $v_v$  is the volume fraction of voids/porosity in the composite,  $m_m$  and  $m_p$  are the poisson's ratios of the matrix and particulates, and  $k(v_p)$  is the slope of the tensile strength against the mean particle size (diameter) and is a function of particle volume fraction  $v_p$ . The computed tensile strength values are within the permissible bounds of the experimental results as shown in Figure 12.

### Elastic Modulus

Elastic modulus is a measure of the stiffness of a material. Anisotropy prevails in many composites. Silicon carbide (SiC) is much stiffer than 7020 aluminium alloy.

Kerner (1956) found equation for estimating the modulus of a composite that contains spherical particles in a matrix as follows:



$$E_c = E_m \left( 1 + \frac{v_p}{1 - v_p} \frac{15(1 - m_m)}{8 - 10m_m} \right) \quad (12)$$

for  $E_p \geq E_m$  and  $m_m$  is the matrix poisson's ratio.  $V_p$  is the volume fraction;  $E_m$  is the elastic modulus of the matrix.

Counto (1964) proposed a simple model for a twophase particulate composite by assuming perfect bonding between particle and matrix. The elastic modulus of the composite is given by

$$\frac{1}{E_c} = \frac{1 - v_p^{1/2}}{E_m} + \frac{1}{\left(1 - v_p^{1/2}\right) / v_p^{1/2} E_m + E_p} \quad (13)$$

where  $v_p$  is the elastic modulus of SiC<sub>p</sub>.

Ishai & Cohen(1967) developed based on a uniform stress applied at the boundary, the elastic modulus of the composite is given by

$$\frac{E_c}{E_m} = 1 + \frac{1 + (\delta - 1)v_p^{2/3}}{1 + (\delta - 1)(v_p^{2/3} - v_p)} \quad (14)$$

which is upper-bound equation. They assumed that the particle and matrix are in a state of macroscopically homogeneous and adhesion is perfect at the interface. The lower-bound equation is given by

$$\frac{E_c}{E_m} = 1 + \frac{v_p}{\delta / (\delta - 1) - v_p^{1/3}} \quad (15)$$

where  $\delta = E_p / E_m$ .

The Young's modulus of particulate composites with the modified rule of mixtures is given by Fu et al. (2002):

$$E_c = \chi_p E_p v_p + E_m (1 - v_p) \quad (16)$$

Where  $0 < \chi_p < 1$  is a particulate strengthening factor.

The proposed equation by the author to find elastic modulus includes the effect of voids/porosity in the composite as given below:

$$\frac{E_c}{E_m} = \left( \frac{1 - v_v^{2/3}}{1 - v_v^{2/3} + v_v} \right) + \left( \frac{1 + (\delta - 1)v_p^{2/3}}{1 + (\delta - 1)(v_p^{2/3} - v_p)} \right) \quad (17)$$

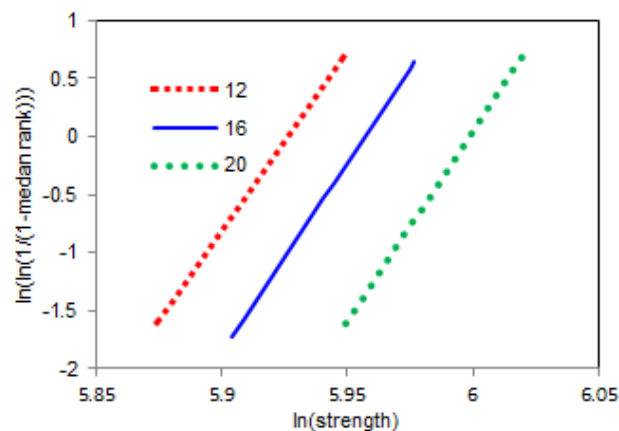
where  $v_v$  is the volume fraction of voids/porosity in the composite. The elastic moduli computed from the above criteria are registered in table 1. The values of elastic moduli obtained from the proposed expression are nearly equal to those of Ishai and Cohen criteria.

**Table 1: Elastic Modulus Obtained from Various Criteria**

Criteria	Young's Modulus, Gpa		
	V <sub>p</sub> =12	V <sub>p</sub> =16	V <sub>p</sub> =20
Kerner	86.84	92.69	99.12
Counto	110.32	120.17	130.43
Ishai and Cohen (upper bound)	169.90	177.34	184.78
Ishai and Cohen (lower bound)	84.11	89.31	95.04
Rule of mixture (modified)	88.05	93.36	98.68
New proposal by Authors	168.43	175.38	182.31

### Weibull Statistical Strength Criterion

The tensile strength of 7020/SiCp was analyzed by Weibull statistical strength criterion using Microsoft Excel software. 7020/SiCp composite indicates increasing failure rate ( $\beta$  values much higher than 1.0). The Weibull graphs of tensile strength indicate lesser reliability for volume fractions of 12% than those reliabilities of 16%, and 20% (Figure 13). The shape parameters,  $\beta$ s (gradients of graphs) are 30.82, 32.52, and 32.78 respectively, for the composites having the particle volume fraction of 12%, 16%, and 20%.

**Figure 13: Weibull Distribution of Tensile Strength**

The Weibull characteristic strength is a measure of the scale in the distribution of data. It so is happened that  $\sigma_0$  equals the strength at which 63.2 percent of the composite has failed. With 7020/SiCp, about 36.8 percent of the tensile specimens should survive at least 374.85 MPa, 386.54 MPa, and 402.89 MPa for 12%, 16%, and 20% volume fractions of SiCp in the specimens respectively. The reliability graphs of tensile strength are shown in Figure 14. At reliability 0.90 the survival tensile strength of 7020/SiCp containing 12% of volume fraction is 348.45 MPa, 16% of volume fraction is 366.69 MPa, and 20% of volume fraction is 376.15 MPa.

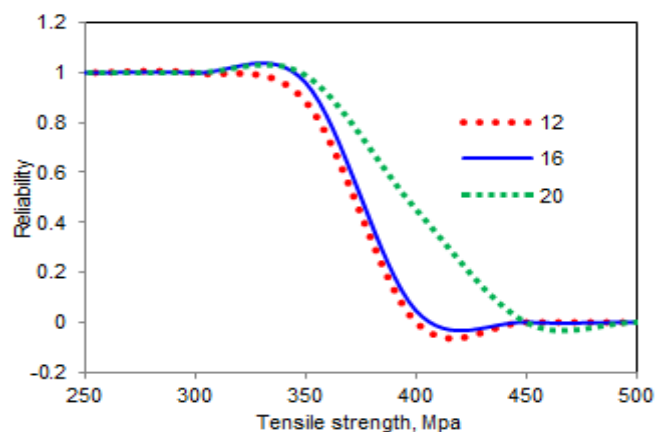


Figure 14: Reliability Graphs for Tensile Strength of 7020/SiC<sub>p</sub>

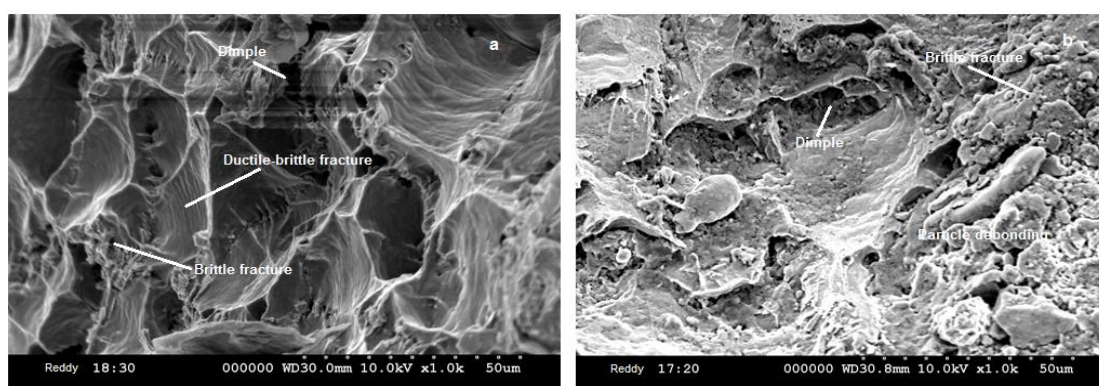


Figure 15: SEM of Fracture Surface of 7020/SiC Composites (a) of 20% Vp and 800nm Particle Size (b) of 20% Vp and 20 μm Particle Size

## Fracture

The failure path in these composites is from the matrix through the matrix/particle interface to the particles. The cracking of SiC particles was a rare event for small size ( $\leq 10\mu\text{m}$ ) of particles as cited by Sugimura & Suresh (1992). The ductile-brittle fracture is observed in the composite consisting of 20% volume fraction and 800nm particle size of SiC as shown in Figure 15a. The clustering is also observed in this composite because the small size SiC reinforcement particles reduces the average distance in the composite to form clustering and to act as strong barriers to dislocation motion. The brittle fracture is observed in the composite consisting of 20% volume fraction and 20 μm particle size of SiC as shown in Figure 15b. Reddy (2002) has established that the void coalescence occurs when the void elongates to the initial intervold spacing. The dimpled appearance of the fractured surfaces is observed in all the composites.

## CONCLUSIONS

The EDS report confirms the presence of  $\text{MgZn}_2$  and  $\text{Mg}_2\text{Si}$  precipitates in the 7020/SiC<sub>p</sub> composites. The porosity of approximately  $36\mu\text{m}$  was observed in the 7020/SiC<sub>p</sub> composite having 20μm particles. At higher volume fractions and small size particles, the particle-particle interaction may develop agglomeration in the composite. Non-planar cracking of particle was observed in the 7020/SiC<sub>p</sub> composite comprising 20μm particles. The tensile strength increases with increase in volume fraction of SiC<sub>p</sub>, whereas it decreases with increasing particle size. The fracture mode was ductile-brittle in nature.

## REFERENCES

1. Counto, U. J. (1964), Effect of the elastic modulus, creep and creep recovery of concrete, Magazine of Concrete Research, 16, 129-138.
2. Fu, S. Y, Xu, G, Mai, T. W. (2002), On the elastic modulus of hybrid, particle/short fiber/polymer composites, Composite Part B, 33, 291-299.
3. Hashim, J, Looney, L, & Hashmi, M. S. J. (2001), The enhancement of wettability of SiC particles in cast aluminum matrix composites, Journal of Materials Processing, 119, 329-335.
4. Hojo, H, Toyoshima, W, Tamura, M, & Kawamura, N. (1974), Short- and long- term strength characteristics of particulate-filled cast epoxy resin, Polymer Engineering & Science, 14, 604-609.
5. Ishai, O, & Cohen, I. J. (1967), Elastic properties of filled and porous epoxy composites, International Journal of Mechanical Sciences, International Journal of Mechanical Sciences, 9, 539-546.
6. Kerner, E. H. (1956), The elastic and thermoelastic properties of composite media, Proceedings of the Physical Society B, 69, 808-813.
7. Landon, G, Lewis, G, & Boden, G. (1977) The influence of particle size on the tensile strength of particulate-filled polymers, Journal of materials Science, 12, 1605-1613.
8. Laurent, V, Chatain, D, & Eustathopoulos, N. (1987), Wettability of SiC by aluminium and Al-Si alloys, Journal of Materials Science, 22, 224-230.
9. Lee, J. C, Subramanian, K. N, & Y. Kim. (1994), The interface in  $\text{Al}_2\text{O}_3$  particulate-reinforced aluminium alloy composite and its role on the tensile Properties, Journal of Materials Science, 29, 1983-1990.
10. Lloyd, D. J. (1991), Aspects of particle fracture in particulate reinforced MMCs, Acta Materialia, 39, 59-72.
11. Prakash, O, Sang, H, & Embury, J. D. (1995), Structure and properties of Al-SiC foam, Materials Science and Engineering, A199, 195-203.
12. Punkanszky, B, Turcsanyi, B, & Tudos, F.(1998) Interfaces in polymer, ceramic and metal matrix composites (Edited by Ishida H, Amsterdam, Elsevier, 467-477.
13. Reddy, A. C. (2002), Influence of ageing, inclusions and voids on ductile fracture mechanism in commercial Al-alloys, Indian Journal of Engineering & Material Sciences, 5, 365-368.
14. Reddy, A. C. (2002), Fracture behavior of brittle matrix and alumina trihydrate particulate composites, Indian Journal of Engineering & Materials Sciences, 5, 365-368.
15. Reddy, A. C. (2009), Mechanical properties and fracture behavior of 7020/SiCp Metal Matrix Composites Fabricated by Low Pressure Die Casting Process, Journal of Manufacturing Technology Research, 1, 273-286.
16. Reddy, A. C, &Essa Zitoun.(2010), Tensile behavior Of 6063/ $\text{Al}_2\text{O}_3$  particulate metal matrix composites fabricated by investment casting process, International Journal of Applied Engineering Research, 1, 542-552.
17. Reddy, A. C, &Essa Zitoun.(2011), Tensile properties and fracture behavior of 7020/ $\text{Al}_2\text{O}_3$  metal matrix

- composites fabricated by low pressure die casting process, *International Journal of Materials Sciences*, 06, 147-157.
18. Reddy, A. C. (2011), Strengthening mechanisms and fracture behavior of 7072Al/Al<sub>2</sub>O<sub>3</sub> metal matrix composites, *International Journal of Engineering Science and Technology*, 03, 6090-6100.
  19. Reddy, A. C. (2011), Evaluation of mechanical behavior of Al-alloy/Al<sub>2</sub>O<sub>3</sub> metal matrix composites with respect to their constituents using Taguchi, *International Journal of Emerging Technologies and Applications in Engineering Technology and Sciences*, 04, 26-30.
  20. Reddy, A. C. (2011), Tensile fracture behavior of 7072/SiC<sub>p</sub> metal matrix composites fabricated by gravity die casting process, *Materials Technology: Advanced Performance Materials*, 26, 257-262.
  21. Reddy, A. C. (2011), Evaluation of mechanical behavior of Al-alloy/SiC metal matrix composites with respect to their constituents using Taguchi techniques, *i-manager's Journal of Mechanical Engineering*, 01, 31-41.
  22. Rohatgi, P. K., Asthana, R, & Das, S. (1986), Solidification, Structures and Properties of Cast Metal-Ceramic Particle Composites, *International Material Reviews*, 31, 115-139.
  23. Sugimura, Y, & Suresh, S. (1992), Effects of SiC content on fatigue crack growth in aluminium alloy reinforced with SiC particles, *Metallurgical Transactions*, 23A, 2231-2342.
  24. Vaucher, S, & Beffort, O. (2001), Bonding and interface formation in metal matrix composites, MMC-Assess – Thematic Network, MMC-Assess Consortium, 1-41.
  25. Whitehouse, A. F, & Clyne, T. W. (1993), Cavity formation during tensile straining of particulate and short fiber metal matrix composites, *Acta Materialia*, 41, 1701-1711.

